

Large-Scale Spectrum Allocation for Cellular Networks via Sparse Optimization

Binnan Zhuang, Dongning Guo, *Senior Member, IEEE*, Ermin Wei, and Michael L. Honig, *Fellow, IEEE*

Abstract—This paper studies joint spectrum allocation and user association in large heterogeneous cellular networks. The objective is to maximize some network utility function based on given traffic statistics collected over a slow timescale, conceived to be seconds to minutes. A key challenge is scalability: interference across cells creates dependencies across the entire network, making the optimization problem computationally challenging as the size of the network becomes large. A suboptimal solution is presented, which performs well in networks consisting of one hundred access points (APs) serving several hundred user devices. This is achieved by optimizing over local overlapping neighborhoods, defined by interference conditions, and by exploiting the sparsity of a globally optimal solution. Specifically, with a total of k user devices in the entire network, it suffices to divide the spectrum into k segments, where each segment is mapped to a particular set, or *pattern*, of active APs within each local neighborhood. The problem is then to find a mapping of segments to patterns, and to optimize the widths of the segments. A convex relaxation is proposed for this, which relies on a re-weighted ℓ_1 approximation of an ℓ_0 constraint, and is used to enforce the mapping of a unique pattern to each spectrum segment. A distributed implementation based on alternating direction method of multipliers (ADMM) is also proposed. Numerical comparisons with benchmark schemes show that the proposed method achieves a substantial increase in achievable throughput and/or reduction in the average packet delay.

Index Terms—Alternating direction method of multipliers (ADMM), convex optimization, resource allocation, small cells, spectrum management, wireless networks.

I. INTRODUCTION

Heterogeneous cellular networks with densely deployed access points (APs) have been proposed for Long Term Evolution Advanced (LTE-A) [1]–[3], and are anticipated to be key components of 5G networks. The deployment of such dense networks brings new challenges with interference management. Mitigating inter-cell interference, in particular, requires coordinated radio resource allocation across multiple cells. Methods that operate over fast timescales include multi-cell joint scheduling [4]–[6] and dynamic spectrum allocation methods associated with orthogonal frequency-division multiple access (OFDMA) [7]–[12], in combination with power control and beamforming.

The assignment of mobiles to APs, or user association, can also take into account the interference environment. Those methods include assigning the user to the strongest AP and the

range extension techniques [13], [14] for balancing the load between macro and pico tiers, along with more sophisticated optimizations of an overall utility objective [15]–[20].

This paper considers the joint optimization of resource allocation and user association in a large network with many APs. The objective is to optimize a network utility, such as average delay, given traffic statistics and average channel state information that change slowly over a geographic region. Our approach builds upon the *slow*-timescale optimization framework proposed in [21], [22]. “Slow” refers to timescales over which average packet arrival and departure rates are relatively stationary. The timescale is conceived to be seconds to minutes in current networks. Given a network of n APs and k mobile devices, the spectrum is partitioned into 2^n *patterns*, corresponding to all possible subsets of active APs [21]. The problem, as originally formulated in [21], is then to optimize the widths of spectrum segments, corresponding to the different patterns, along with the association of patterns with devices. The solution has been shown to provide significant performance improvement in throughput enhancement, delay reduction, and energy savings [21]–[27].

Although it was shown in [21] and [22] that the solution is *sparse* (at most k out of 2^n patterns have nonzero bandwidth), finding the set of optimal patterns that appear in the solution is in general NP-hard. In prior work [23], we have proposed a scalable approach to finding an approximate solution by recognizing that each link rate depends only on a *local pattern*, containing only those APs within an *interference cluster*. The problem can then be redefined over sets of overlapping clusters, associated with those local patterns. Each AP has its own interference cluster, which captures the interference from nearby APs. Additional constraints are needed to ensure that the spectrum assigned to each particular AP is consistent across all clusters to which it belongs. Even with those constraints, however, the convex optimization may not find consistent *placements* of the spectrum segments for all APs within the available band. A discrete coloring algorithm is proposed in [23] to ensure that the local patterns are globally consistent. In this way, the total number of variables is reduced from $O(2^n)$ in [21] to polynomial in n , facilitating scalability.

In this paper, we take a different approach to address the scalability problem, which exploits the fact that there exists a globally optimal solution that contains at most k active patterns. Specifically, we reformulate the problem by dividing the spectrum into k segments, and attempt to identify the pattern that should be associated with each segment. This effectively reverses the approach in [23], which attempts to assign a segment of spectrum to each pattern. In this reformulation, we initially allow any combination of patterns

B. Zhuang was with the Department of Electrical Engineering and Computer Science at Northwestern University, Evanston, IL, 60208. He is now with Samsung Semiconductor, Inc., Modem R&D Lab, San Diego, CA. D. Guo, E. Wei and M. L. Honig are with the Department of Electrical Engineering and Computer Science at Northwestern University, Evanston, IL, 60208.

This work was supported in part by a gift from Futurewei Technologies and by the National Science Foundation under Grant No. CCF-1423040.

that can be assigned to each of the k segments. This problem is a convex relaxation of the original problem. The one-to-one mapping of spectrum segments to patterns is then enforced with an ℓ_0 (cardinality) constraint. An algorithm for finding an approximate solution to this problem is presented based on a reweighted ℓ_1 approximation of the ℓ_0 constraint [28].

The approach to scalability presented here has the following advantages relative to the approach in [23]. First, it effectively trades the combinatorial coloring problem that arises in [23] with the ℓ_0 constraint introduced here. Although this does not simplify the original problem, it helps in finding an approximate solution, since reweighted ℓ_1 approximations for the ℓ_0 norm have been known to perform well. Second, the number of variables is reduced from $O(2^n)$ in [23] to $O(nk)$, facilitating scalability. Third, the numerical results presented here indicate that this method generally gives better performance for a fixed computational complexity than the method in [23]. Decomposing the centralized iterative algorithm into subproblems based on the alternating direction method of multipliers (ADMM) [29], we also develop a distributed solution.

In related work [30], the problem is to select an active set of links (equivalently, a pattern) on a particular time slot (equivalently, a frequency band) in a peer-to-peer network to maximize a weighted sum rate. An iterative algorithm based on fractional programming determines a *single* pattern for each time slot. In contrast, we jointly optimize the patterns and their bandwidths. Kuang et al [24] considered a similar framework for optimizing spectrum allocation and user association, where the search set is limited to a small number of patterns *a priori* to avoid the combinatorial complexity.

The rest of the paper is organized as follows. The system model is presented in Section II. The original formulation with 2^n global patterns is presented in Section III. A scalable formulation with a sparsity constraint is presented in Section IV. An efficient centralized iterative algorithm for finding an approximate solution is presented in Section V and a distributed algorithm based on ADMM is presented in Section VI. Simulation results are presented in Section VII. Concluding remarks are given in Section VIII.

II. SYSTEM MODEL

In a network with n APs, we denote the set of AP indices as $N = \{1, \dots, n\}$. The n APs share W Hz of spectrum (treated as one unit), which can be considered homogeneous on a slow timescale. (All segments of the resource have the same quality.) The notion of resource can also be generalized to time (scheduling) and the combination of spectrum and time (resource block allocation in the time-frequency grid). We focus on one time period on the slow timescale. Each AP can transmit on any part(s) of the spectrum. Hence, each slice of the spectrum can be shared by any subset of APs. We refer to the 2^n possible ways (subsets of n APs) to share a slice of the spectrum as *patterns*, each corresponding to a subset $A \subset N$. If a slice of spectrum is designated to pattern A , only APs in A can transmit over the spectrum and they interfere at the devices they serve. Due to spectrum homogeneity, it suffices to describe an allocation of the spectrum to APs as

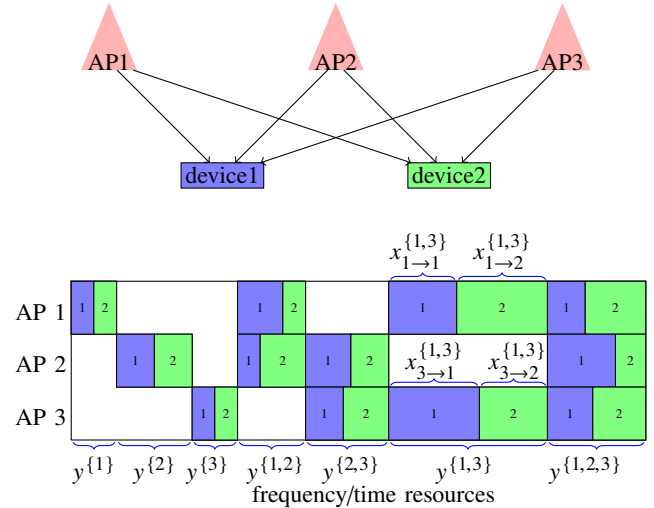


Fig. 1. Illustration of all patterns of a 3-AP 2-mobile network with spectrum allocation variables.

$\{y^A\}_{A \subset N}$, where y^A denotes the fraction of total bandwidth allocated to pattern A . The total bandwidth allocated to all patterns (including the empty set \emptyset) is one unit:

$$\sum_{A \subset N} y^A = 1. \quad (1)$$

An example with three APs and two devices is depicted in Fig. 1. AP 1 exclusively owns the spectrum allocated to pattern $\{1\}$; shares the spectrum allocated to pattern $\{1, 2\}$ with AP 2; shares the spectrum allocated to pattern $\{1, 3\}$ with AP 3; and shares the spectrum allocated to pattern $\{1, 2, 3\}$ with both AP 2 and AP 3.

In principle, a device may be served by any subset of APs and an AP may serve any subset of devices. In practice, however, a device is only served by APs within a small neighborhood around it. This is because the channel gain from a transmitter to a receiver vanishes quickly with the distance between them. Let $K = \{1, \dots, k\}$ denote the set of k device indices. Let $E \subset N \times K$ denote the set of (admissible) links from APs to devices. The APs, mobile devices, and links in E form a bipartite graph with APs on one side and devices on the other. Device j can only be served by the set of neighboring APs in this bipartite graph, denoted by set

$$A_j = \{i \in N \mid (i \rightarrow j) \in E\}, \quad (2)$$

where $i \rightarrow j$ denotes the link from AP i to device j . Likewise, AP i can only serve its set of neighboring devices, denoted by

$$U_i = \{j \in K \mid (i \rightarrow j) \in E\}. \quad (3)$$

Evidently, $i \in A_j$ if and only if $j \in U_i$. Since an isolated AP or device in the graph should not be assigned any resource at an efficient spectrum allocation, we assume no terminal is isolated without loss of generality, i.e., the sets A_j and U_i are nonempty.

When $i \in A \cap A_j$, we use $x_{i \rightarrow j}^A$ to denote the fraction of total bandwidth used by AP i to serve device j under pattern A . (Several such x -variables are illustrated in Fig. 1.) Note that we do not define the variable if $i \notin A$ (AP i does not transmit under

pattern A) or $i \notin A_j$ (AP i cannot serve device j). Although we could equivalently set the variable to zero whenever $i \notin A \cap A_j$, we simply omit those variables. We assume that an AP uses orthogonal (non-overlapping) spectrum to serve different devices. Since the total bandwidth assigned to pattern A is y^A , we have:

$$\sum_{j \in U_i} x_{i \rightarrow j}^A = y^A, \quad \forall A \subset N, i \in A. \quad (4)$$

For $i \in A \cap A_j$, let $s_{i \rightarrow j}^A$ denote the *value* of the link from AP i to device j per unit of resource under pattern A . Again, the parameter is undefined if $i \notin A \cap A_j$ (as opposed to setting it to zero). For concreteness, we let the coefficient $s_{i \rightarrow j}^A$ represent the spectral efficiency of link $i \rightarrow j$ under pattern A . We assume that when AP i transmits over any part(s) of the spectrum, it transmits with fixed flat power spectral density (PSD) p_i .¹ The parameter $s_{i \rightarrow j}^A$ is determined by the pathloss and shadowing of link $i \rightarrow j$, and characteristics of the interference links from other APs in A to device j . In this paper, we assume that when a device decodes information from one AP's signals over a slice of spectrum, it treats all interference over the same spectrum as noise.² For concreteness, we use Shannon's formula to write:

$$s_{i \rightarrow j}^A = W \log_2 \left(1 + \frac{p_i g_{i \rightarrow j}}{\sum_{i' \in A \setminus \{i\}} p_{i'} g_{i' \rightarrow j} + n_j} \right), \quad \forall i \in A \cap A_j \quad (5)$$

in bits per second, where $g_{i \rightarrow j}$ denotes the (slow-timescale average) power gain of link $i \rightarrow j$, and n_j is the noise PSD at device j . With this definition the total data rate for device j is then given by

$$r_j = \sum_{A \subset N} \sum_{i \in A \cap A_j} s_{i \rightarrow j}^A x_{i \rightarrow j}^A, \quad \forall j \in K. \quad (6)$$

Both the spectral efficiency and the service rate represent averages over the slow timescale.

Given a specific allocation, if AP i transmits to device j under at least one pattern, i.e., $i \in A_j$ and $\sum_{A \subset N: i \in A} x_{i \rightarrow j}^A > 0$, then they are said to be *associated* with each other.

III. PROBLEM FORMULATION USING GLOBAL PATTERNS

The objective of the slow-timescale optimization is to maximize a network utility function over the spectrum allocation across all links and patterns represented by $\mathbf{x} = (x_{i \rightarrow j}^A)_{A \subset N, i \in A, j \in U_i}$. Let $u(r_1, \dots, r_k)$ denote a network utility function of the rate tuple $\mathbf{r} = [r_1, \dots, r_k]$. In each time period,

the optimization problem with constraints (1), (4), and (6) is formulated as P0:

$$\text{maximize}_{\mathbf{r}, \mathbf{x}, \mathbf{y}} u(r_1, \dots, r_k) \quad (\text{P0a})$$

$$\text{subject to } r_j = \sum_{A \subset N} \sum_{i \in A \cap A_j} s_{i \rightarrow j}^A x_{i \rightarrow j}^A, \quad \forall j \in K \quad (\text{P0b})$$

$$\sum_{j \in U_i} x_{i \rightarrow j}^A = y^A, \quad \forall A \subset N, i \in A \quad (\text{P0c})$$

$$\sum_{A \subset N} y^A = 1 \quad (\text{P0d})$$

$$x_{i \rightarrow j}^A \geq 0, \quad \forall A \subset N, i \in A, j \in U_i. \quad (\text{P0e})$$

Since all the constraints are linear, the optimization problem is convex if $u(\mathbf{r})$ is concave in the service rate vector \mathbf{r} . The class of utility functions that make P0 convex include the frequently-used (weighted) sum rate, the sum log-rate, and the minimum user rate, among others.

For concreteness, we follow [23] and focus on minimizing the average packet delay. Specifically, we assume homogeneous Poisson packet arrivals for device j at rate λ_j and exponentially distributed packet lengths of τ bits on average. The service rate r_j/τ (in packets/second) is sustainable for serving device j 's queue regardless of the state of other devices' queues. In this case, device j 's queueing dynamics are precisely modeled by an M/M/1 queue. The average packet sojourn time is given by

$$\frac{1}{(r_j/\tau - \lambda_j)^+} \quad (7)$$

where $1/x^+ = 1/x$ if $x > 0$ and $1/x^+ = +\infty$ if $x \leq 0$.³ The network utility function can be expressed as:

$$u(r_1, \dots, r_k) = - \sum_{j=1}^k \frac{\lambda_j}{(r_j/\tau - \lambda_j)^+}. \quad (8)$$

The traffic arrival rates and spectral efficiencies are updated once each period on the slow timescale. P0 is intended to be solved once each period on a slow timescale. The optimized patterns are used throughout the decision period of seconds or minutes. In fact, the notion of a device on such a slow timescale can be considered as a set of service requests from the same geographic area, which share the same quality of service (QoS) (due to the same long-term average spectral efficiencies). The pattern based spectrum allocation determines the spectrum needed to serve different types of service requests (from different locations). Thus, slow timescale spectrum allocation complements fast time resource allocation, i.e., implemented over a period measured in milliseconds. The interaction of the two timescales are discussed in [27].

It is instructive to count the number of variables in P0. It is not difficult to see that there are k r -variables, 2^n y -variables, and the number of x -variables is

$$2^{n-1} \sum_{i=1}^n |U_i| \quad (9)$$

¹Power control will be considered in future work.

²The framework can be generalized to treat many forms of coordinated multipoint (CoMP) transmissions. For example, cooperative transmission is considered in [31].

³Unlike $1/x$, the function $1/x^+$ is convex on $(-\infty, \infty)$ and is recognized as such by many optimization software packages. We therefore write $1/x^+$ instead of $1/x$, which is nonconvex on $(-\infty, \infty)$ with the constraint $x > 0$.

where $|\cdot|$ yields the cardinality of a set. Even if the number of devices any AP can serve is upper bounded by a constant k_0 (i.e., $|U_i| \leq k_0, \forall i \in N$), the total number of variables in P0 is on the order of $O(n2^n)$. This suggests that, even though P0 is convex, it is very hard to solve directly for all but a small number of APs.

To make progress, we shall use the following fact that P0 admits a sparse optimal solution:

Proposition 1: ([22]) If the utility function $u(\mathbf{r})$ of P0 is concave in the rate vector \mathbf{r} , then there exists a $(k+1)$ -sparse optimal allocation, namely, an optimal solution that satisfies:

$$|\{A \subset N \mid y^A > 0\}| \leq k+1. \quad (10)$$

Furthermore, if the utility function is element-wise nondecreasing in the rate vector, then there exists a k -sparse optimal solution.

By Proposition 1, it suffices to identify no more than $k+1$ out of the 2^n patterns to activate. This property is the key to the scalable algorithm developed in the next section.

IV. REFORMULATION WITH SPARSITY CONSTRAINTS

Solving P0 directly is prohibitively expensive for large networks due to the inherit complexity from the exponential number of patterns, referred to as *global patterns* in the sequel. Although Proposition 1 guarantees the existence of a sparse optimal solution, it remains computationally difficult to determine a small subset of active patterns at an optimal solution out of the 2^n possible patterns. In this section, we introduce the notion of *local pattern* and a relaxation to significantly reduce the number of variables. We then exploit the sparse structure of the optimal solution to derive a scalable formulation.

A. Local Pattern

The key idea is to approximate the link spectral efficiency under a global pattern by that under a local pattern, where the APs outside the local pattern (referred to as remote APs) are treated as stationary noise sources, whose on/off dynamics can be ignored. For device j , its *local patterns* consist of all subsets of its neighborhood A_j . Here we assume all remote APs ($N \setminus A_j$) are always on, and generate interference. This gives the pessimistic approximation

$$\tilde{s}_{i \rightarrow j}^A = s_{i \rightarrow j}^{A \cup (N \setminus A_j)}, \quad \forall i \in A \cap A_j. \quad (11)$$

That is, the spectral efficiency is regarded to be identical to that under the global pattern $A \cup (N \setminus A_j)$, which includes all remote APs. In contrast, an optimistic approximation is defined by ignoring all remote interference: $\tilde{s}_{i \rightarrow j}^A = s_{i \rightarrow j}^{A \cap A_j}$, $\forall i \in A \cap A_j$. There are, of course, other possibilities in between, e.g., reducing the amount of interference from remote APs according to their utilizations. We note that if the neighborhoods are sufficiently large, so that remote APs' total interference is negligible compared to thermal noise, then the preceding approximations are arbitrarily accurate. Indeed, if all links outside the set E have zeros gains, then the approximations become precise. In this paper, we adopt

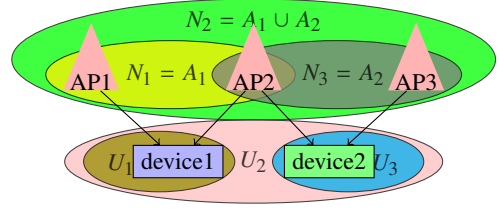


Fig. 2. Neighborhoods in the case of three APs and two devices.

the pessimistic assumption (11) for the numerical results in Section VII.

In the sequel, we abuse the notation slightly to redefine $s_{i \rightarrow j}^A$ in the case where A does not include all remote APs:

$$s_{i \rightarrow j}^A = s_{i \rightarrow j}^{A \cup (N \setminus A_j)}, \quad \text{if } i \in A \cap A_j \text{ and } N \setminus A_j \not\subset A. \quad (12)$$

Evidently, (12) degrades those redefined efficiencies in general. Moreover, those redefined spectral efficiencies are equal to the corresponding local ones defined in (11). We henceforth use the notation $s_{i \rightarrow j}^A$ to represent the (redefined) spectral efficiencies under both global patterns ($A \subset N$) and local patterns ($A \subset A_j$). A consequence of (12) is that the spectral efficiency now depends only on the local pattern:

$$s_{i \rightarrow j}^A = s_{i \rightarrow j}^{A \cap A_j}, \quad \forall i \in A \cap A_j. \quad (13)$$

B. Local Allocation Variables

We next introduce a set of local allocation variables, which shall be used to replace the original $O(n2^n)$ (global) variables. Let us define the *interference cluster (or cluster)* of AP i as:

$$N_i = \cup_{j \in U_i} A_j, \quad (14)$$

which includes AP i itself and all APs that may directly interfere with it. Fig. 2 depicts an example with three APs and two devices. The set of admissible links are $E = \{1 \rightarrow 1, 2 \rightarrow 1, 2 \rightarrow 2, 3 \rightarrow 2\}$. Therefore, the AP neighborhoods are $U_1 = \{1\}$, $U_2 = \{1, 2\}$, and $U_3 = \{2\}$; and the device neighborhoods are $A_1 = \{1, 2\}$ and $A_2 = \{2, 3\}$. The interference cluster of AP 1 is $N_1 = \{1, 2\}$, as AP 2 interferes with it at device 1. The interference cluster of AP 3 is $N_3 = \{2, 3\}$, as AP 2 interferes with it at device 2. The interference cluster of AP 2 is $N_2 = \{1, 2, 3\}$, since AP 1 and AP 3 interfere with it at device 1 and device 2, respectively.

In what follows, we assume that an AP serves at most k_0 devices and each device is served by at most n_0 APs, i.e., $|A_j| \leq n_0$ for all $j \in K$ and $|U_i| \leq k_0$ for all $i \in N$, where k_0 and n_0 are constants. Thus the bipartite graph has finite node degrees. This implies an upper bound on the cluster sizes:

$$|N_i| \leq k_0 n_0, \quad \forall i \in N. \quad (15)$$

We next rewrite the service rates defined in (6) in terms of a new set of *local* allocation variables. Although the spectral efficiency of link $i \rightarrow j$ only depends on local patterns in the device neighborhood, A_j , the local allocation variables at AP i are defined over all subsets of interference cluster N_i . This is because two local allocations in their respective interference clusters must be consistent over the overlapping area of the

clusters, as shall be illustrated shortly. Specifically, for every admissible link $(i \rightarrow j) \in E$ and every subset B of the cluster N_i with $i \in B$, let

$$z_{i \rightarrow j}^B = \sum_{A \subset N: A \cap N_i = B} x_{i \rightarrow j}^A, \quad (16)$$

which represents the total bandwidth allocated to the link under all global patterns that match the local pattern B . The total number of z -variables is:

$$\sum_{i \in N} |U_i| 2^{|N_i|-1} \leq nk_0 2^{k_0 n_0} \quad (17)$$

which grows linearly with the network size n . For every $j \in K$, the service rate defined in (6) and (P0b) can be calculated as:

$$r_j = \sum_{i \in A_j} \sum_{A \subset N: i \in A} s_{i \rightarrow j}^A x_{i \rightarrow j}^A \quad (18)$$

$$= \sum_{i \in A_j} \sum_{B \subset N_i: i \in B} s_{i \rightarrow j}^B \sum_{A \subset N: A \cap N_i = B} x_{i \rightarrow j}^A \quad (19)$$

$$= \sum_{i \in A_j} \sum_{B \subset N_i: i \in B} s_{i \rightarrow j}^B z_{i \rightarrow j}^B \quad (20)$$

where (19) follows from $s_{i \rightarrow j}^A = s_{i \rightarrow j}^{A \cap A_j} = s_{i \rightarrow j}^{A \cap N_i \cap A_j} = s_{i \rightarrow j}^{B \cap A_j} = s_{i \rightarrow j}^B$ whenever $A_j \subset N_i$ and $A \cap N_i = B$,⁴ and (20) is due to definition (16). The service rate r_j now depends on no more than $O(n)$ z -variables in (20) in lieu of $O(n2^n)$ x -variables in (6).

C. An Equivalent Formulation

In this subsection, we reformulate P0 as an equivalent optimization problem using $O(kn)$ ‘‘local’’ variables in lieu of the $O(n2^n)$ global variables. This is in part motivated by the sparsity property guaranteed by Proposition 1, i.e., there exists an optimal solution with at most $k + 1$ active patterns. We reformulate the problem by dividing the spectrum into $k + 1$ segments with the goal that each segment eventually corresponds to one pattern to activate. The service rate to device j is rewritten as:

$$r_j = \sum_{l \in L} \sum_{i \in A_j} \sum_{B \subset N_i: i \in B} s_{i \rightarrow j}^B z_{i \rightarrow j}^{B,l}, \quad \forall j \in K \quad (21)$$

where $L = \{0, \dots, k\}$ is the index set of the $k + 1$ segments. Basically, each $z_{i \rightarrow j}^B$ defined in (16) is replicated $k + 1$ times as $(z_{i \rightarrow j}^{B,0}, \dots, z_{i \rightarrow j}^{B,k})$ for the $k + 1$ segments. There are altogether $O(kn)$ such $z_{i \rightarrow j}^{B,l}$ variables.

We also introduce a set of local variables to take the place of the global y -variables. Specifically, for every $l \in L$, $i \in N$, and $B \subset N_i$, let $y_i^{B,l}$ denote the total bandwidth assigned to AP i 's local pattern, $B \subset N_i$, within segment l . Then, in analogy to (P0c), we have

$$\sum_{j \in U_i} z_{i \rightarrow j}^{B,l} = y_i^{B,l}, \quad \forall l \in L, i \in N, B \subset N_i: i \in B. \quad (22)$$

⁴One may replace $s_{i \rightarrow j}^B$ by $s_{i \rightarrow j}^{B \cap A_j}$ in (20) to save storage needed for the spectral efficiency parameters. We use $s_{i \rightarrow j}^B$ for ease of notation.

Let h^l denote the bandwidth assigned to segment l , where $\sum_{l \in L} h^l = 1$. Evidently, the total bandwidth allocated to all local patterns of AP i within segment l should equal h^l :

$$\sum_{B \subset N_i} y_i^{B,l} = h^l, \quad \forall i \in N, l \in L. \quad (23)$$

To enforce a one-to-one mapping of the $k + 1$ active patterns to segments, we add the following constraint, which allows at most one local pattern to be activated in each interference cluster within each segment:

$$\sum_{B \subset N_i} |y_i^{B,l}|_0 \leq 1, \quad \forall i \in N, l \in L \quad (24)$$

where the ℓ_0 -norm is defined as $|x|_0 = 1$ if $x \neq 0$, and $|x|_0 = 0$ if $x = 0$.

Collecting the preceding constraints, we introduce the following problem formulation, referred to as P1:

$$\text{maximize}_{r, y, z} u(r_1, \dots, r_k) \quad (\text{P1a})$$

$$\text{subject to } r_j = \sum_{i \in A_j} \sum_{B \subset N_i: i \in B} s_{i \rightarrow j}^B \sum_{l \in L} z_{i \rightarrow j}^{B,l}, \quad \forall j \in K \quad (\text{P1b})$$

$$\sum_{j \in U_i} z_{i \rightarrow j}^{B,l} = y_i^{B,l}, \quad \forall l \in L, i \in N, B \subset N_i: i \in B \quad (\text{P1c})$$

$$\begin{aligned} \sum_{B \subset N_i: B \cap N_m = C} y_i^{B,l} &= \sum_{B \subset N_m: B \cap N_i = C} y_m^{B,l}, \\ \forall l \in L, i, m \in N: N_i \cap N_m &\neq \emptyset \\ \forall C \subset N_i \cap N_m: C &\neq \emptyset \end{aligned} \quad (\text{P1d})$$

$$\sum_{B \subset N_i} y_i^{B,l} = h^l, \quad \forall l \in L, i \in N \quad (\text{P1e})$$

$$\sum_{B \subset N_i} |y_i^{B,l}|_0 \leq 1, \quad \forall l \in L, i \in N \quad (\text{P1f})$$

$$z_{i \rightarrow j}^{B,l} \geq 0, \quad \forall l \in L, i \in N, j \in U_i, B \subset N_i \quad (\text{P1g})$$

$$\sum_{l \in L} h^l = 1 \quad (\text{P1h})$$

where (P1b), (P1c), (P1e), and (P1f) are identical to (21)–(24). The additional constraint (P1d) was introduced in [23] to ensure consistency of bandwidth allocations across overlapping clusters. Basically, for every nonempty local pattern $C \subset N_i \cap N_m$, the total bandwidth allocated to C in the interference cluster of AP i must be identical to the total bandwidth allocated to C in the interference cluster of AP m . As an example, consider the network depicted in Fig. 2. In interference cluster N_1 , AP 2 transmits under pattern $\{2\}$ and $\{1, 2\}$; while in interference cluster N_3 , AP 2 transmits under pattern $\{2\}$ and $\{2, 3\}$. The overlapping pattern is $C = \{2\}$. Since the same physical spectrum is allocated to AP 2 whether viewed in cluster N_1 or N_3 , we have $y_1^{\{2\},l} + y_1^{\{1,2\},l} = y_3^{\{2\},l} + y_3^{\{2,3\},l}$.

We prove the following equivalence in Appendix.

Theorem 1: If (13) holds, then the global formulation P0 and the local formulation P1 are equivalent in the sense that they achieve the same maximum utility with the same optimal

rate vectors. In addition, given an optimal solution to P1, the optimal global patterns to activate are

$$B^l = \bigcup_{i \in N} \bigcup_{B \subset N_i; y_i^{B,l} > 0} B, \quad l \in L \quad (25)$$

and the corresponding solution to P0 is given by

$$x_{i \rightarrow j}^A = \sum_{l: A=B^l} z_{i \rightarrow j}^{B^l, l}, \quad \forall A \in N, i \in A, j \in U_i. \quad (26)$$

The detailed proof of Theorem 1 is shown in the Appendix.

V. ITERATIVE ℓ_1 APPROXIMATION

The number of variables is reduced from $O(n2^n)$ in P0 to $O(kn)$ in P1. However, the ℓ_0 norm constraint makes the problem non-convex and difficult to solve using standard solvers. In this section, we propose a reweighted ℓ_1 constraint in lieu of the ℓ_0 norm constraint to obtain a sparse solution. This approach was previously proposed in [28] to address an ℓ_0 norm in the optimization objective and has been applied to various problems in the literature. The basic idea here is to use the weighted ℓ_1 norm, $\sum_i w_i |y_i|$ as a local approximation of the ℓ_0 norm $\sum_i |y_i|_0$ in constraint (P1f), where w_i is updated in each iteration to be inversely proportional to the current ℓ_1 norm, $|y_i|$. The intuition is to discourage small nonzero entries with large weights.

Because the ℓ_0 norm constraints on different segments are related through (P1e) and (P1h), the ℓ_1 heuristic cannot be directly applied to P1. We develop an iterative algorithm based on the ℓ_1 reweighted heuristic, where the weights depend on both the ℓ_1 norm and the bandwidth allocated to each segment h^l . In each iteration of Algorithm 1, we solve the following optimization problem:

$$\underset{r, y, z}{\text{maximize}} \quad u(r_1, \dots, r_k) \quad (P2a)$$

$$\text{subject to} \quad \sum_{B \subset N_i} w_i^{B,l} y_i^{B,l} \leq 1, \quad \forall l \in L, \forall i \in N \quad (P2b)$$

$$(P1b), (P1c), (P1d), (P1e), (P1g), (P1h).$$

The only difference from P1 is that we substitute the ℓ_0 norm constraint (P1f) with the weighted sum (P2b)⁵.

The iterative algorithm for solving P2 is described as Algorithm 1. At the initial stage, a random initialization of the weights is used to introduce the necessary asymmetry in the first iteration. Otherwise, e.g., setting all $w_i^{B,l} = 1$, the solution will be symmetric over all segments, which is not optimal in general. In each iteration, we solve P2 with the current weights w to obtain the corresponding optimal x, y, z and $h = [h^0, \dots, h^k]$. Then the weights are updated. The iteration terminates when the solution converges or the maximum number of iterations t_{max} ⁶ is reached.

The weight update in Algorithm 1 is designed to approximate the ℓ_0 norm (see [28] and the reference therein). Because we want to keep searching over all local patterns, μh^l is added to the denominator, with $\mu \in (0, 1)$. Note that we use

⁵Since $y_i^{B,l} \geq 0$ due to (P1c) and (P1g), the ℓ_1 norm is equivalent to the weighted sum.

⁶The maximum number of iterations is limited to 8 in our simulations.

Algorithm 1 Iterative algorithm with reweighted ℓ_1 approximation.

INPUT: $(s_{i \rightarrow j}^B)_{j \in K, i \in A_j, B \subset N_i}$, and $(\lambda_j)_{j \in K}$.

OUTPUT: The bandwidths allocated to the $k+1$ segments $(h^l)_{l \in L}$, the $k+1$ active patterns $(B^l)_{l \in L}$, and the spectrum allocated to link $i \rightarrow j$ on segment l , $(\bar{x}_{i \rightarrow j}^l)_{j \in K, i \in A_j, l \in L}$

Initialization: Randomly choose $w_i^{B,l} \in (0, 1)$, $i \in N$, $B \subset N_i$, $l \in L$, $\mu \in (0, 1)$.

Repeat

1. Solve P2, with the current weights w .
2. Update $w_i^{B,l} = (y_i^{B,l} + \mu h^l)^{-1}$, $\forall i \in N$, $B \subset N_i$, $l \in L$.
3. $t = t + 1$.

until $(y_i^{B,l})_{i \in N, B \subset N_i, l \in L}$ converges or the maximum number of iteration is reached.

Post Processing:

4. For all $l \in L$, determine the optimal local patterns:

$$B_i^l = \arg \max_{B \subset N_i} y_i^{B,l}, \quad (27)$$

and the corresponding global pattern:

$$B^l = \cup_{i \in N} B_i^l. \quad (28)$$

5. For segment $l \in L$, the spectral efficiency of link $i \rightarrow j$ becomes:

$$\bar{s}_{i \rightarrow j}^l = \begin{cases} s_{i \rightarrow j}^{B^l \cap A_j}, & \text{if } B^l \cap A_j \neq \emptyset, \\ 0, & \text{otherwise.} \end{cases} \quad (29)$$

6. Optimize $(\bar{x}_{i \rightarrow j}^l)_{j \in K, i \in A_j, l \in L}$ by solving the following optimization problem:

$$\underset{\bar{x}, h}{\text{maximize}} \quad u(r_1, \dots, r_k) \quad (P3a)$$

$$\text{subject to} \quad r_j = \sum_{l \in L} \sum_{i \in A_j} \bar{s}_{i \rightarrow j}^l \bar{x}_{i \rightarrow j}^l, \quad \forall j \in K \quad (P3b)$$

$$\sum_{j \in U_i} \bar{x}_{i \rightarrow j}^l = h^l, \quad \forall l \in K \quad (P3c)$$

$$\sum_{l \in L} h^l = 1 \quad (P3d)$$

$$\bar{x}_{i \rightarrow j}^l \geq 0, \quad \forall i \in N, j \in U_i, l \in L. \quad (P3e)$$

a variable μh^l unlike the fixed ϵ proposed in [28], which adapts to the bandwidth h^l change in different iterations. Algorithm 1 simultaneously searches for the optimal pattern on each segment as well as the bandwidth allocated to it. While the heuristic of iteratively approximating ℓ_0 by reweighted ℓ_1 norms lacks formal convergence guarantees, it performs well in practice as observed in [28].

A consensus on a single pattern may not be reached for all segments when the iterations terminate. We use (27) to enforce a unique pattern on each segment by letting AP i use a dominating pattern. The unified global pattern B^l on segment l is thus given by the union of all the dominating patterns on segment l , which is shown in (28). Given the $k+1$ global patterns, we can determine the spectral efficiency for each link

$(i \rightarrow j)$ under those patterns provided by (29)⁷. The bandwidth of all segments, $\mathbf{h} = (h^l)_{l \in L}$ and the spectrum allocation over different links on each segment, $\bar{\mathbf{x}} = (\bar{x}_{i \rightarrow j}^l)_{j \in K, i \in A_j, l \in L}$ are further optimized by solving the relatively simple problem P3 in Algorithm 1 with $O(nk)$ variables.

One way of using Algorithm 1 to solve P1 is by passing the required parameters to a central controller to optimize the spectrum allocation and user association. The required parameters are channel information $(s_{i \rightarrow j}^B)_{j \in K, i \in A_j, B \subset N_i}$ and traffic information $(\lambda_j)_{j \in K}$. These parameters are static and only need to be communicated once in each time period. Hence, the number of coefficients sent to the central controller is $O(k)$. The optimal solution obtained using Algorithm 1 can be represented by the optimal patterns $(B^l)_{l \in L}$, the optimal bandwidths of the segments $(h^l)_{l \in L}$, and the allocation variables $(\bar{x}_{i \rightarrow j}^l)_{j \in K, i \in A_j, l \in L}$, which is much less than the number of variables originally in P1. Thus, the central controller only needs to feed back $O(k^2)$ variables to inform the optimal allocation to the APs.

VI. A DISTRIBUTED ALGORITHM BASED ON ADMM

ADMM originates from the augmented Lagrangian algorithm [32], [33]. It solves a problem with decomposable objective by iteratively solving small sub-problems and reconciling their results. The ADMM has been proved to be effective in solving many optimization problems that arise from “big data”. ADMM based solutions can often be implemented in a distributed manner or make use of parallel computing to solve subproblems simultaneously. In the previous section, we introduced P2 as a convex approximation of P1. Here we show how to use an ADMM based algorithm to solve the convex problem P2 in a distributed way.

We first present an equivalent formulation of P2:

$$\underset{\mathbf{r}, \mathbf{z}, \mathbf{y}}{\text{maximize}} \quad u(r_1, \dots, r_k) \quad (\text{P4a})$$

$$\text{subject to} \quad v_{i,m}^{C,l} = \sum_{B \subset N_i: B \cap N_m = C} y_i^{B,l},$$

$$\forall l \in L, m, i \in N, C \subset N_i \cap N_m : C \neq \emptyset \quad (\text{P4b})$$

$$v_{i,m}^{C,l} = v_{m,i}^{C,l},$$

$$\forall l \in L, m, i \in N, C \subset N_i \cap N_m : C \neq \emptyset \quad (\text{P4c})$$

$$(\text{P1b}), (\text{P1c}), (\text{P1e}), (\text{P1g}), (\text{P1h}), (\text{P2b}).$$

The additional auxiliary variables $(v_{i,m}^{C,l})_{i,m \in N, l \in L, C \subset N_i \cap N_m: C \neq \emptyset}$ are for decomposing the optimization problem into subproblems, which consist of only local variables.

The augmented Lagrangian of P4 can be written as:

$$L(\mathbf{v}, \mathbf{y}, \mathbf{z}, \mathbf{h}, \boldsymbol{\alpha}, \boldsymbol{\beta}, \boldsymbol{\gamma}) = \sum_{j \in K} u_j(r_j) - \boldsymbol{\alpha}^T (\mathbf{y} - \mathbf{Fz})$$

$$- \frac{\rho}{2} (\mathbf{y} - \mathbf{Fz})^T (\mathbf{y} - \mathbf{Fz}) - \boldsymbol{\beta}^T (\mathbf{v} - \mathbf{Gy}) - \boldsymbol{\gamma}^T (\mathbf{Hy} - \mathbf{h}) \quad (30)$$

$$- \frac{\rho}{2} (\mathbf{v} - \mathbf{Gy})^T (\mathbf{v} - \mathbf{Gy}) - \frac{\rho}{2} (\mathbf{Hy} - \mathbf{h})^T (\mathbf{Hy} - \mathbf{h}),$$

⁷Since one pattern is used in each segment, the spectral efficiency is determined for each segment.

where the rate variables r_j is calculated by (P1b), and $\mathbf{v}, \mathbf{y}, \mathbf{z}$ and \mathbf{h} are the vectors containing all $v_{i,m}^{C,l}, y_i^{B,l}, z_{i \rightarrow j}^{B,l}$, and h^l variables, respectively. $\boldsymbol{\alpha}, \boldsymbol{\beta}$, and $\boldsymbol{\gamma}$ are the Lagrangian multipliers for the constraints (P1c), (P4b) and (P1e), respectively. In (30), the constraints (P1c), (P4b) and (P1e) are written in vector form as $\mathbf{y} - \mathbf{Fz} = 0$, $\mathbf{v} - \mathbf{Gy} = 0$, and $\mathbf{Hy} - \mathbf{h} = 0$, respectively. The positive parameter ρ controls the weight on the quadratic penalty terms, which also corresponds to the step size of the dual descent update in the ADMM based solution to be introduced. We only consider the dual variables of the equality constraints (P1c), (P4b), and (P1e) in (30). The rest of the constraints are omitted here for simplicity, which will be considered when solving each subproblem.

Algorithm 2 The ADMM based algorithm.

INPUT: $\boldsymbol{\lambda} = [\lambda_1, \dots, \lambda_k]^T$, $\mathbf{s} = (s_{i \rightarrow j}^B)_{j \in K, i \in A_j, B \subset N_i}$, $\mathbf{w} =$

$(w_i^{B,l})_{l \in L, i \in N, B \subset N_i}$

OUTPUT: $\mathbf{v}, \mathbf{y}, \mathbf{z}$ and \mathbf{h}

Initialize $\mathbf{v}_0, \mathbf{z}_0, \mathbf{h}_0, \boldsymbol{\alpha}_0, \boldsymbol{\beta}_0, \boldsymbol{\gamma}_0$ and set $t = 0$.

while \mathbf{y}, \mathbf{z} and \mathbf{h} have not converged and $t < t_{max}$ **do**

$$\mathbf{y}_{t+1} = \arg \max_{\mathbf{y}} L(\mathbf{v}_t, \mathbf{y}, \mathbf{z}_t, \mathbf{h}_t, \boldsymbol{\alpha}_t, \boldsymbol{\beta}_t, \boldsymbol{\gamma}_t)$$

$$[\mathbf{z}_{t+1}; \mathbf{v}_{t+1}; \mathbf{h}_{t+1}] = \arg \max_{\mathbf{z}, \mathbf{v}, \mathbf{h}} L(\mathbf{v}, \mathbf{y}_{t+1}, \mathbf{z}, \mathbf{h}, \boldsymbol{\alpha}_t, \boldsymbol{\beta}_t, \boldsymbol{\gamma}_t)$$

$$\boldsymbol{\alpha}_{t+1} = \boldsymbol{\alpha}_t + \rho(\mathbf{y}_{t+1} - \mathbf{Fz}_{t+1})$$

$$\boldsymbol{\beta}_{t+1} = \boldsymbol{\beta}_t + \rho(\mathbf{v}_{t+1} - \mathbf{Gy}_{t+1})$$

$$\boldsymbol{\gamma}_{t+1} = \boldsymbol{\gamma}_t + \rho(\mathbf{Hy}_{t+1} - \mathbf{h}_{t+1})$$

$$t = t + 1$$

end while

An ADMM based iterative algorithm is shown in Algorithm 2 to solve P2. The algorithm takes any initialization. In each iteration, there are three steps to update the primal and dual variables. First, update \mathbf{y}_{t+1} based on $\mathbf{v}_t, \mathbf{z}_t, \mathbf{h}_t, \boldsymbol{\alpha}_t, \boldsymbol{\beta}_t$ and $\boldsymbol{\gamma}_t$ calculated from the previous iteration to minimize (30). Then, update $\mathbf{v}_{t+1}, \mathbf{z}_{t+1}$ and \mathbf{h}_{t+1} based on $\mathbf{y}_{t+1}, \boldsymbol{\alpha}_t, \boldsymbol{\beta}_t$ and $\boldsymbol{\gamma}_t$. The dual variables $\boldsymbol{\alpha}_{t+1}, \boldsymbol{\beta}_{t+1}$ and $\boldsymbol{\gamma}_{t+1}$ are updated at the end of each iteration with the newly updated primal variables.

We next explain the distributed computation and message sharing used in the preceding updates. The update of \mathbf{y} can be decomposed into n subproblems associated with each of the n APs. Define the part of the augmented Lagrangian (30) related to \mathbf{y} as:

$$L_{[\mathbf{y}]}(\mathbf{v}_t, \mathbf{y}, \mathbf{z}_t, \mathbf{h}_t, \boldsymbol{\alpha}_t, \boldsymbol{\beta}_t, \boldsymbol{\gamma}_t) =$$

$$- \boldsymbol{\alpha}_t^T (\mathbf{y} - \mathbf{Fz}_t) - \frac{\rho}{2} (\mathbf{y} - \mathbf{Fz}_t)^T (\mathbf{y} - \mathbf{Fz}_t)$$

$$- \boldsymbol{\beta}_t^T (\mathbf{v}_t - \mathbf{Gy}) - \frac{\rho}{2} (\mathbf{v}_t - \mathbf{Gy})^T (\mathbf{v}_t - \mathbf{Gy}) \quad (31)$$

$$- \boldsymbol{\gamma}_t^T (\mathbf{Hy} - \mathbf{h}_t) - \frac{\rho}{2} (\mathbf{Hy} - \mathbf{h}_t)^T (\mathbf{Hy} - \mathbf{h}_t)$$

where $\mathbf{v}_t, \mathbf{x}_t, \mathbf{h}_t, \boldsymbol{\alpha}_t, \boldsymbol{\beta}_t$ and $\boldsymbol{\gamma}_t$ are obtained in the previous iteration. The subproblem associated with AP i is obtained by

taking the part of (31) that depends on $\mathbf{y}_i = (y_i^{B,l})_{B \in N_i, l \in L}$:

$$\begin{aligned} \text{minimize}_{\mathbf{y}_i} & \sum_{l \in L} \sum_{B \subset N_i; i \in B} (y_i^{B,l} - \sum_{j \in U_i} z_{i \rightarrow j}^{B,l} + \frac{\alpha_i^{B,l}}{\rho})^2 \\ & + \sum_{l \in L} \sum_{m \in N_i} \sum_{C \subset N_i \cap N_m; C \neq \emptyset} (v_{i,m}^{C,l} - \sum_{B \subset N_i; B \cap N_m = C} y_i^{B,l} + \frac{\beta_{i,m}^{C,l}}{\rho})^2 \\ & + \sum_{l \in L} (\sum_{B \subset N_i} y_i^{B,l} - h^l + \frac{\gamma_i^l}{\rho})^2 \end{aligned} \quad (\text{Py a})$$

$$\text{subject to} \quad \sum_{B \subset N_i} w_i^{B,l} y_i^{B,l} \leq 1, \quad \forall l \in N, \quad (\text{Py b})$$

which requires intermediate results: $\alpha_{i,t} = (\alpha_i^{B,l})_{l \in L, B \subset N_i; i \in B}$, $\beta_{i,t} = (\beta_{i,m}^{C,l})_{l \in L, m \in N_i, C \subset N_i \cap N_m; C \neq \emptyset}$, $\gamma_{i,t} = (\gamma_i^l)_{l \in L}$, $\mathbf{h}_t = (h^l)_{l \in L}$, $\mathbf{v}_{i,t} = (v_{i,m}^{C,l})_{l \in L, m \in N_i, C \subset N_i \cap N_m; C \neq \emptyset}$, and $\mathbf{z}_{i,t} = (z_{i \rightarrow j}^{B,l})_{l \in L, j \in U_i, B \subset N_i}$. We shall see that $\alpha_{i,t}$, $\beta_{i,t}$, $\mathbf{v}_{i,t}$, and $\gamma_{i,t}$ are updated locally at AP i , when introducing the corresponding subproblems. The variables in $\mathbf{z}_{i,t}$ are updated at the devices in U_i . Hence, the information sharing due to $\mathbf{z}_{i,t}$ is within AP i 's local cluster U_i . Only \mathbf{h} are shared globally, which requires sharing $k+1$ real numbers in each iteration of Algorithm 2.

The update of \mathbf{z} , \mathbf{v} and \mathbf{h} in Algorithm 2 can be divided into the updates of \mathbf{z} , \mathbf{v} , and \mathbf{h} , respectively. The part of (30) relates to \mathbf{z} is:

$$L_{\mathbf{z}}(\mathbf{z}, \mathbf{y}_{t+1}, \boldsymbol{\alpha}_t) = \sum_{j \in K} u_j(r_j) - \boldsymbol{\alpha}_t^T (\mathbf{y}_{t+1} - \mathbf{F}\mathbf{z}) - \frac{\rho}{2} \|\mathbf{y}_{t+1} - \mathbf{F}\mathbf{z}\|^2. \quad (32)$$

The subproblem for $\mathbf{z}_j = (z_{i \rightarrow j}^{B,l})_{i \in A_j, B \subset N_i, l \in L}$ is given by:

$$\text{maximize}_{\mathbf{z}_j} u_j(r_j) - \sum_{l \in L} \sum_{i \in A_j} \sum_{B \subset N_i; i \in B} (y_i^{B,l} - \sum_{j \in U_i} z_{i \rightarrow j}^{B,l} + \alpha_i^{B,l} / \rho)^2 \quad (\text{Pz a})$$

$$\text{subject to} \quad r_j = \sum_{i \in A_j} \sum_{B \subset N_i; i \in B} s_{i \rightarrow j}^B \sum_{l \in L} z_{i \rightarrow j}^{B,l} \quad (\text{Pz b})$$

$$z_{i \rightarrow j}^{B,l} \geq 0, \quad \forall l \in L, i \in N, B \subset N_i. \quad (\text{Pz c})$$

The constraints (Pz b) and (Pz c) contain only the parts of (P1b) and (P1g) for \mathbf{z}_j , respectively. The message sharing includes $\mathbf{y}_{j,t} = (y_i^{B,l})_{l \in L, i \in A_j, B \subset N_i; i \in B}$ and $\boldsymbol{\alpha}_{j,t} = (\alpha_i^{B,l})_{l \in L, i \in A_j, B \subset N_i; i \in B}$, which are updated and shared by the APs in device j 's local cluster A_j . The rest of the \mathbf{z} variables in (Pz a) are updated at devices that can be served by the same APs as device j , i.e., devices in U_i such that $i \in A_j$. To emphasize the association of the variable \mathbf{z}_j and subproblem Pz to device j , we say the subproblem is solved at device j . However, in practice, the problem should be physically solved at an AP instead, e.g., the nearest AP to device j .

The variable \mathbf{v} can be separately updated for each pair of $v_{i,m}^{C,l}$ and $v_{m,i}^{C,l}$ in (P4c). If we initialize with $\beta_{i,m}^{C,l} + \beta_{m,i}^{C,l} = 0$, it

is easy to prove that the \mathbf{v} update is in the following closed form:

$$\begin{aligned} v_{i,m}^{C,l} &= v_{m,i}^{C,l} \\ &= \frac{1}{2} \left(\sum_{B: B \cap N_m = C, B \subset N_i} y_{i,t+1}^{B,l} + \sum_{B: B \cap N_i = C, B \subset N_m} y_{m,t+1}^{B,l} \right). \end{aligned} \quad (33)$$

The computation in (34) can be taken in parallel at different APs, i.e., AP i updates $(v_{i,m}^{C,l})_{l \in L, m \in N_i, C \subset N_i \cap N_m; C \neq \emptyset}$. To compute (34), $(y_{i,m}^{B,l})_{B: B \cap N_m = C, B \subset N_i}$ is available at AP i and $(y_{m,i}^{B,l})_{B: B \cap N_i = C, B \subset N_m}$ is updated at AP i 's interferer, AP m . Therefore, the message sharing is locally among AP i and its interfering APs in N_i .

The subproblem for solving \mathbf{h} is:

$$\text{minimize}_{\mathbf{h}} \sum_{i \in N} \sum_{l \in L} \left(\sum_{B \subset N_i} y_i^{B,l} - h^l + \gamma_i^l / \rho \right)^2 \quad (\text{Ph a})$$

$$\text{subject to} \quad h^l \geq 0, \quad \forall l \in L \quad (\text{Ph b})$$

$$\sum_{l \in L} h^l = 1, \quad (\text{Ph c})$$

which can be easily solved with standard quadratic programming solver, since it only has $k+1$ variables. To solve Ph, each AP i needs to pass $(\sum_{B \subset N_i} y_i^{B,l})_{l \in L}$ and $(\gamma_i^l)_{l \in L}$, i.e., $2(k+1)$ real values, to a central controller for the computation.

The update of dual variable $\boldsymbol{\alpha}$ can be obtained in distributed manner at the n APs:

$$\alpha_i^{B,l} = \alpha_i^{B,l} + \rho \left(y_i^{B,l} - \sum_{j \in U_i} z_{i \rightarrow j}^{B,l} \right), \quad \forall l \in L, B \subset N_i; i \in B, \quad (35)$$

where $\mathbf{y}_{i,t+1} = (y_i^{B,l})_{B \in N_i, l \in L}$ is updated locally at AP i and $\mathbf{z}_{i,t+1} = (z_{i \rightarrow j}^{B,l})_{l \in L, j \in U_i, B \subset N_i}$ are provided by the devices in U_i .

Analogously, $\boldsymbol{\beta}$ is updated at the n APs:

$$\begin{aligned} \beta_{i,m}^{C,l} &= \beta_{i,m}^{C,l} + \rho \left(v_{i,m}^{C,l} - \sum_{B \subset N_i; B \cap N_m = C} y_i^{B,l} \right), \\ \forall l \in L, m \in N_i, C \subset N_i \cap N_m; C \neq \emptyset, \end{aligned} \quad (36)$$

where both $\mathbf{y}_{i,t+1} = (y_i^{B,l})_{B \in N_i, l \in L}$ and $\mathbf{v}_{i,t+1} = (v_{i,m}^{C,l})_{l \in L, m \in N_i, C \subset N_i \cap N_m; C \neq \emptyset}$ are updated at AP i as explained above.

The $\boldsymbol{\gamma}$ update can also be performed at the n APs:

$$\gamma_i^l = \gamma_i^l + \rho \left(\sum_{B \subset N_i} y_i^{B,l} - h^l \right), \quad \forall l \in L, \quad (37)$$

where $\mathbf{y}_{i,t+1}^l = (y_i^{B,l})_{B \in N_i, l \in L}$ is locally available, and $\mathbf{h}_{t+1} = (h^l)_{l \in L}$ are broadcasted to all APs.

The updates in Algorithm 2 are divided into simple subproblems that can be solved in distributed manner for each AP or device. Only local message sharing is required during this process, except broadcasting the $k+1$ values $(h^l)_{l \in L}$ from

TABLE I
PARAMETER CONFIGURATIONS.

Parameter	Value/Function
pathloss exponent	3
standard deviation of shadow fading	3
macro transmit PSD	5 μ W/Hz
pico transmit PSD	1 μ W/Hz
noise PSD	1×10^{-7} μ W/Hz
total bandwidth	20 MHz
average packet length	1 Mb

the central controller to the n APs, and receiving the $2(k+1)$ values $\left(\sum_{B \subset N_i} y_i^{B,l}\right)_{l \in L}$ and $(\gamma_i^l)_{l \in L}$ at the central controller from each AP i . The above distributed updates of Algorithm 2 can also be used for parallel computing by passing the required information to a cloud.

The ADMM based Algorithm 2 solves the convex optimization step in each iteration of Algorithm 1, which takes up most of the computational cost. Here, we also want to point out that the weights updates $w_i^{B,l} = (y_i^{B,l} + \mu h^l)^{-1}$ can also be carried out at each AP i . Even for the very simple post processing P3, we can derive a distributed solution based on ADMM. Therefore, the entire Algorithm 1 can be implemented in a distributed manner. Since ADMM has been shown to converge to the optimal solution for any convex problem [29], the proposed method inherits the same convergence guarantee. The suboptimal solution achieved by Algorithm 1 is due to approximating ℓ_0 norm using reweighted ℓ_1 norm.

VII. NUMERICAL RESULTS

The solution obtained by Algorithm 1 is evaluated using numerical simulations. Unless specified otherwise, the general assumptions are given as follows: Among the n APs, one macro AP is located at the center of the area and $n-1$ pico APs are randomly dropped around it. The k devices are assumed to be located on k randomly chosen lattice points in the network. Both distance based pathloss and shadowing are considered to obtain the link gains. The common parameters used for all the simulations in this section are shown in Table I.

A. Performance in Small Networks

We compare the solutions to P0 and P1 in a small network cluster with $n = 10$ and $k = 23$. Since the number of variables is not too large in this case, we solve both versions of P0 with and without the local neighborhood approximation (13) using a standard convex optimization solver. The solution to P1 is obtained using iterative l_1 reweighted algorithm in Algorithm 1. To solve P1, we can either compute the update in each iteration of Algorithm 1 with a standard convex optimization solver or use the ADMM based distributed algorithm in Algorithm 2. The local neighborhoods are constructed by considering the strongest four APs for each device. Two other simple schemes are also compared here. One is the full spectrum allocation with the maxRSRP association. The other is the optimal orthogonal allocation,⁸ i.e., the solution

⁸Both spectrum allocation and user association are optimized assuming each AP exclusively occupies a fraction of the spectrum.

to P0 under the additional assumption that only the singleton patterns $\{1\}, \{2\}, \dots, \{n\}$ are active.

The delay versus traffic arrival rate curves are shown in Fig. 3. The rightmost end of each curve represents the maximum arrival rate can be supported by the corresponding allocation scheme. The optimal orthogonal allocation (marked by circle marker) quickly becomes saturated, as the orthogonal spectrum allocation is very inefficient even only orthogonalizing over 10 APs. The full spectrum allocation with maxRSRP association (without any marker) achieves much higher throughput. However, the delay also increases with respect to the optimal orthogonal allocation as all APs cause interference to each other. The curves obtained by solving P0 with and without local neighborhood approximation are very close, which indicates considering the four strongest interferers and treating interference from remote APs as noise is accurate enough in the network setup. The solution to P1 obtained by general convex solver and the ADMM based algorithm are almost on top of each other, which proves the validity of the ADMM based solution. Hence, in the subsequent results, we will only show the solution obtained using a standard convex solver in Algorithm 1. The solutions to P1 achieve slightly longer delay than the solutions to P0. The maximum packet arrival rates that can be supported by the solutions to P0 and P1 are the same. For all the simulations in this section, we limit the maximum number of iterations in Algorithm 1 to eight. The jointly optimized spectrum allocation and user association achieves substantial delay reduction as well as eight times throughput compared to the simple full spectrum allocation with maxRSRP association.

The optimized spectrum allocations and user associations given by the solutions to P0 (without local neighborhood approximation) and P1 are depicted in Fig. 4a and Fig. 4b, respectively. In Fig. 4, the macro and pico APs are represented by the bigger and smaller towers; each handset represents a device. If a device is associated to an AP, a solid line connects the corresponding AP and the device. The grid on each handset represents the spectrum used by the APs to serve it. The normalized traffic arrival rate (from 0 to 100) of each device is shown under each handset. The allocation achieved by the solution to P0 with local neighborhood approximation is omitted, since it is almost identical to the solution to P0 without local neighborhood approximation. The user association in Fig. 4b is close but not identical to the that in Fig. 4a. This is because the solution to P1 obtained using Algorithm 1 is an approximation to the global optimum with local neighborhood approximation. Take the device on the up left corner as an example, more APs transmit to it using a larger portion of the spectrum in Fig 4b compared to Fig. 4a. This also explains the delay difference between the solution to P0 (with local neighborhood approximation) and the solution to P1 in Fig. 3.

B. Performance in Medium-size Networks

We present the performance comparison of different algorithms in a mid-size network with $n = 30$ APs and $k = 46$ devices, deployed on a 600×600 square meter area. P0 becomes computationally prohibitive due to the 2^{30}

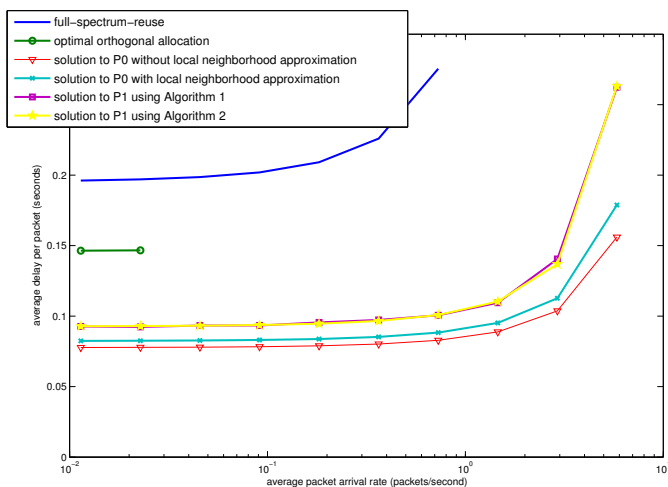


Fig. 3. Delay versus traffic arrival rate curves for a HetNet with $n = 10$ and $k = 23$.

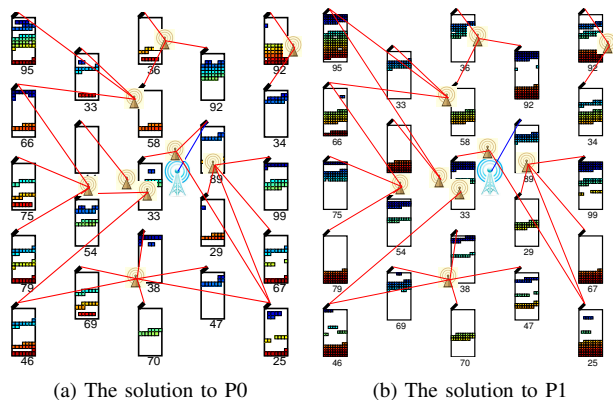


Fig. 4. Proposed spectrum allocations and user associations at traffic arrival rate of 1.46 packets/second.

global patterns. Hence we compare the solution to P1 with the simple maxRSRP association under the full-spectrum-reuse, the optimal orthogonal allocation and the optimal user association under the full-spectrum-reuse. A simplified version of P1 is also compared. Instead of using 46 segments, 5 segments are used, which constrain the solution to no more than five active patterns. The delay versus average traffic arrival rate curves obtained by the five different schemes are shown in Fig. 5. The optimal orthogonal allocation becomes even more inefficient. As the number of APs increases, each AP gets a smaller fraction of the entire spectrum on average. The solutions to P1 using Algorithm 1 still achieves 4 times network throughput and substantial delay reduction compared with the full-spectrum-reuse with maxRSRP association. Interestingly, using 5 segments in P1 achieves almost the same performance as using 46 segments. This is because there are only seven active patterns in the solution to P1 with 46 segments. Many segments use the same active pattern in the solution. Optimizing user association under the full-spectrum-reuse also has superior performance over the full-spectrum-reuse with maxRSRP association. However, it can only support half of the maximum traffic that can be supported by the

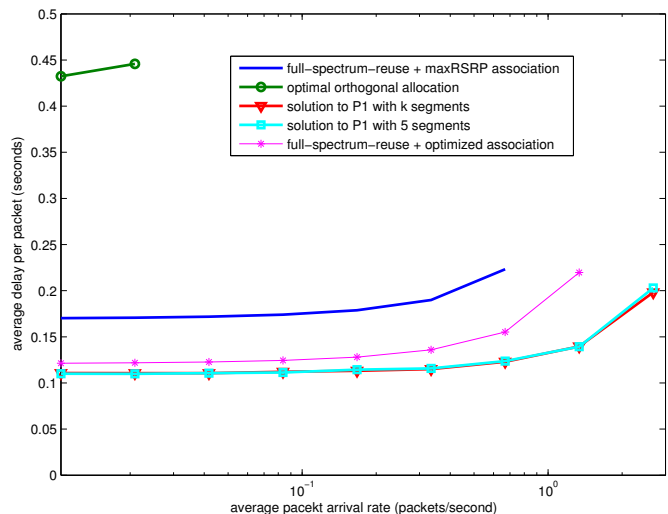


Fig. 5. Delay versus traffic arrival rate curves for a HetNet with $n = 30$ and $k = 46$.

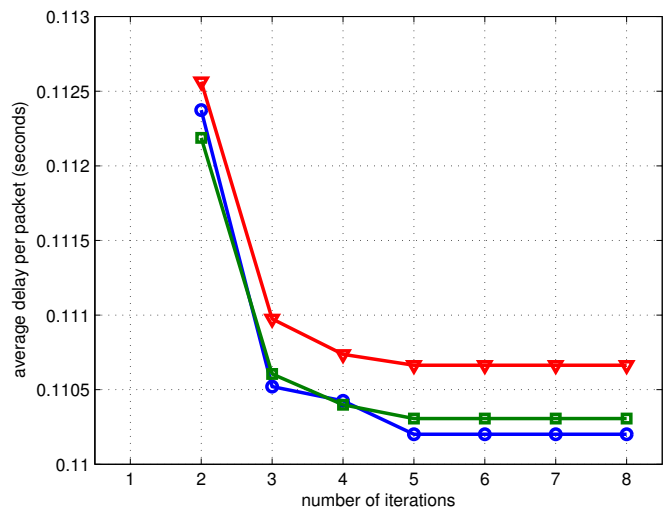


Fig. 6. Delay versus number of iterations in Algorithm 1.

proposed solution.

We also evaluate the convergence behavior of Algorithm 1 using this medium-size network. The average delay versus iteration number curves for the first three traffic loads in Fig. 5 are shown in Fig. 6. To get a feasible spectrum allocation and the corresponding average delay at the end of each iteration, we perform post processing after every iteration. At the end of the first iteration, the dominating pattern on each segment given by (27) is still far from the optimal pattern. Hence, P3 has no feasible solution after the first iteration. That is why no average delay values are shown after the first iteration in Fig. 6. As the iteration continues, Algorithm 1 converges within five iterations under all three traffic loads. In fact, this kind of fast convergence has been observed throughout our simulations.

C. Performance in Large Networks

The performance of different allocation schemes are also compared in a large network with $n = 100$ APs and $k = 200$

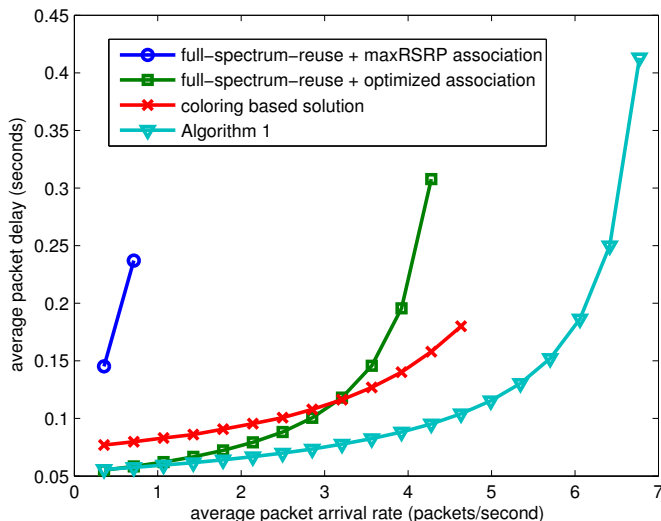


Fig. 7. Delay versus traffic arrival rate curves for a HetNet with $n = 100$ and $k = 200$.

devices, as shown in Fig. 7. The network is deployed on a 1250×1250 square meter area. Here, we want to emphasize a ‘device’ on slow timescales generally represents a class of service requests from different physical devices on fast timescales with the same QoS. Therefore, serving 200 devices on a slow timescale under heavy traffic corresponds to supporting thousands of users on fast timescales. To ease computation, we reduce the sizes of local neighborhoods by constraining each device to be served by the three strongest APs. Under such constraint, the size of interference cluster N_i is mostly between 5 to 8, in the large network.

No optimal orthogonal allocation can support more than the lightest load shown in Fig. 7. Hence, we compare the full-spectrum-reuse with maxRSRP association, the full-spectrum-reuse with optimized association, the coloring based approach in [23], and the solution to P1 obtained using Algorithm 1. The coloring based approach suffers in this very large network due to the suboptimal solution based on various approximations, which is consistent with the observations in [23]. The coloring based solution even achieves higher average delay than the full-spectrum-reuse with optimized association in the light traffic regime. As the load increases, the coloring based approach outperforms the full-spectrum-reuse with optimized association. The proposed solution (Algorithm 1) consistently outperforms all the other three schemes. The throughput gain achieved by Algorithm 1 in this large network is less than that in the medium-size network shown in section VII-B. This is mainly because we only consider the three strongest interferers, which compromises the benefit of interference management.

VIII. CONCLUSION

We have introduced a new aspect of future cellular networks with densely deployed APs through centralized radio resource management. Substantial performance improvement can be achieved by jointly optimizing spectrum allocation and user association across all APs on a slow timescale. Advanced

optimization techniques are used to solve the problem for large networks consisting of many APs and devices. The proposed framework and scalable solution suggest a way for centralized radio resource management on the metropolitan scale. Power control and load dependent interference are not considered in the current problem formulation, which are future research directions.

APPENDIX PROOF OF THEOREM 1

We first present an equivalent formulation of P0 under the local spectral efficiency definition in (13):

Proposition 2: P0 is equivalent to the following problem, P5:

$$\text{maximize}_{r, y, z} u(r_1, \dots, r_k) \quad (\text{P5a})$$

$$\text{subject to } r_j = \sum_{i \in A_j} \sum_{B \subset N_i: i \in B} s_{i \rightarrow j}^B z_{i \rightarrow j}^B, \quad \forall j \in K \quad (\text{P5b})$$

$$z_{i \rightarrow j}^B = \sum_{A \subset N: A \cap N_i = B} x_{i \rightarrow j}^A, \quad \forall i \in N, j \in U_i, B \subset N_i \quad (\text{P5c})$$

$$\sum_{j \in U_i} x_{i \rightarrow j}^A = y^A, \quad \forall A \subset N, i \in A \quad (\text{P5d})$$

$$\sum_{A \subset N} y^A = 1 \quad (\text{P5e})$$

$$x_{i \rightarrow j}^A \geq 0, \quad \forall A \subset N, i \in A, j \in K. \quad (\text{P5f})$$

Proof: To show the equivalence, we only need to prove that (P0b) is equivalent to the combination of (P5c) and (P5b). Under the local neighborhood assumption (13), this is exactly what we have derived in (16) and (18)–(20). \blacksquare

We next prove P1 is equivalent to P5 by introducing two more intermediate equivalent problems.

Proposition 3: P5 is equivalent to the following problem, P6:

$$\text{maximize}_{r, x, y, z} u(r_1, \dots, r_k) \quad (\text{P6a})$$

$$\text{subject to } r_j = \sum_{i \in A_j} \sum_{B \subset N_i} s_{i \rightarrow j}^B \sum_{l \in L} z_{i \rightarrow j}^{B, l}, \quad \forall j \in K \quad (\text{P6b})$$

$$z_{i \rightarrow j}^{B, l} = \sum_{A \subset N: A \cap N_i = B} x_{i \rightarrow j}^A, \quad \forall i \in N, j \in U_i, B \subset N_i, l \in L \quad (\text{P6c})$$

$$\sum_{j \in U_i} x_{i \rightarrow j}^A = y^A, \quad \forall A \subset N, i \in A, l \in L \quad (\text{P6d})$$

$$\sum_{A \subset N} y^A = h^l, \quad \forall l \in L \quad (\text{P6e})$$

$$\sum_{A \in N} |y^A|_0 \leq 1, \quad \forall l \in L \quad (\text{P6f})$$

$$\sum_{l \in L} h^l = 1 \quad (\text{P6g})$$

$$x_{i \rightarrow j}^A \geq 0, \quad \forall A \subset N, i \in A, j \in U_i, l \in L. \quad (\text{P6h})$$

Proof: P6 can be considered as first reformulating P5 by having $k + 1$ constituents of the x, y, z variables for

the $k + 1$ spectrum segments, and then adding the cardinality constraint (P6f) to guarantee one-to-one mapping between active patterns and spectrum segments. We show that every optimal solution to P6 corresponds to an optimal solution to P5, in the sense that they achieve the same rate vector \mathbf{r} as well as the same utility.

First, given an optimal solution to P6, we can combine the variables of the $k + 1$ segments into a feasible solution to P5:

$$z_{i \rightarrow j}^B = \sum_{l \in L} z_{i \rightarrow j}^{B,l}, \quad \forall i \in N, j \in U_i, B \subset N_i \quad (38)$$

$$x_{i \rightarrow j}^A = \sum_{l \in L} x_{i \rightarrow j}^{A,l}, \quad \forall A \subset N, i \in A, j \in U_i \quad (39)$$

$$y^A = \sum_{l \in L} y^{A,l}, \quad \forall A \subset N. \quad (40)$$

It is easy to check the variables \mathbf{x} , \mathbf{y} and \mathbf{z} constructed according to (38), (39), and (40) satisfy all the constraints in P5. According to (P5b) and (P6b), the two solutions also achieve the same rate vector \mathbf{r} , hence also the same utility.

It remains to show that an optimal solution to P5 corresponds to a feasible solution to P6. According to *Theorem 1* and *Proposition 2*, there exists an optimal solution to P5 that activates at most $k + 1$ global patterns y^A . Suppose there are $k' \leq k + 1$ active patterns in such an optimal solution, which is denoted by $A_1, \dots, A_{k'}$. We form a feasible solution to P6 as:

$$h^l = \begin{cases} y^{A_l} & \text{if } l \in \{1, \dots, k'\} \\ 0 & \text{otherwise} \end{cases} \quad (41)$$

$$y^{A,l} = \begin{cases} y^{A_l} & \text{if } l \in \{1, \dots, k'\}, A = A_l \\ 0 & \text{otherwise} \end{cases} \quad (42)$$

$$x_{i \rightarrow j}^{A,l} = \begin{cases} x_{i \rightarrow j}^{A_l} & \text{if } l \in \{1, \dots, k'\}, A = A_l, i \in A, j \in U_i \\ 0 & \text{otherwise.} \end{cases} \quad (43)$$

After obtaining \mathbf{x} by (43), \mathbf{z} can be calculated according to (P6c). We essentially assign the k' active patterns to the first k' segments; and set the bandwidths of the rest of the segments to zero, i.e., $h^l = 0, l = k' + 1, \dots, k + 1$. It is easy to verify that the solution to P6 formed by (41)–(43) satisfies all the constraints in P6 and achieve the same rate tuple \mathbf{r} as the optimal solution to P5.

Therefore, P5 and P6 are equivalent. \blacksquare

Proposition 4: P6 is equivalent to the following problem, P7:

$$\underset{\mathbf{r}, \mathbf{y}, \mathbf{z}}{\text{maximize}} \quad u(r_1, \dots, r_k) \quad (P7a)$$

$$\text{subject to} \quad r_j = \sum_{i \in A_j} \sum_{B \subset N_i} s_{i \rightarrow j}^B \sum_{l \in L} z_{i \rightarrow j}^{B,l}, \quad \forall j \in K \quad (P7b)$$

$$\sum_{j \in U_i} z_{i \rightarrow j}^{B,l} = \sum_{A \subset N: A \cap N_i = B} y^{A,l}, \quad \forall l \in L, i \in N, B \subset N_i \quad (P7c)$$

$$\sum_{A \subset N} y^{A,l} = h^l, \quad \forall l \in L \quad (P7d)$$

$$\sum_{A \subset N} |y^{A,l}|_0 \leq 1, \quad \forall l \in L \quad (P7e)$$

$$y^{A,l} \geq 0, \quad \forall A \subset N, l \in L \quad (P7f)$$

$$z_{i \rightarrow j}^{B,l} \geq 0, \quad \forall i \in N, j \in U_i, B \subset N_i, l \in L \quad (P7g)$$

$$\sum_{l \in L} h^l = 1. \quad (P7h)$$

Proof: Despite the difference between the constraints (P6c), (P6d) and the constraint (P7c), P6 and P7 are equivalent.⁹ Essentially, P7 can be considered as removing the \mathbf{x} variable from P6 and directly relating \mathbf{z} and \mathbf{y} through (P7c). First, we can prove that (P6c) and (P6d) imply (P7c) by:

$$\sum_{j \in U_i} z_{i \rightarrow j}^{B,l} = \sum_{j \in U_i} \sum_{A \subset N: A \cap N_i = B} x_{i \rightarrow j}^{A,l} \quad (44)$$

$$= \sum_{A \subset N: A \cap N_i = B} y^{A,l}, \quad (45)$$

where (44) is due to (P6c); and (45) is due to (P6d). This suggests any solution to P6 is also a feasible solution to P7.

Next, we prove that any solution to P7 also corresponds to a feasible solution to P6. Due to the cardinality constraint (P7e), a feasible solution to P7 has one active global pattern per segment. We denote the active pattern in segment l as B^l , which is defined in (25). The \mathbf{y} and \mathbf{z} variables in a feasible solution to P7 will satisfy all constraints in P6 except (P6c) and (P6d). We then construct $x_{i \rightarrow j}^{A,l}$ in the corresponding solution to P6 as:

$$x_{i \rightarrow j}^{A,l} = \begin{cases} z_{i \rightarrow j}^{B^l \cap N_i, l}, & \text{if } A = B^l \\ 0, & \text{otherwise} \end{cases} \quad (46)$$

for all $i \in N, j \in U_i$, and $A \subset B$. To see that \mathbf{x} constructed according to (46) satisfies (P6c), we only need to prove for the nonnegative variables. The only active local pattern in cluster N_i on segment l is given by $B = B^l \cap N_i$; and the only active global pattern on segment l is $A = B^l$. Hence (P6c) is satisfied due to (46). Given (P7c) and (46), (P6d) directly holds. Therefore, the converse is proved. Hence, P6 and P7 are equivalent. \blacksquare

Proposition 5: P7 is equivalent to P1.

Proof: The difference between P1 and P7 is only in the \mathbf{y} variables, where $y_i^{B,l}$ in P1 is associated with the local pattern $B \subset N_i$, and $y^{A,l}$ in P7 is associated with global pattern $A \subset N$. The objectives of P1 and P7 are identical. The other constraints are equivalent except for constraints (P1c)–(P1f) and (P7c)–(P7e). It remains to show that the two optimization problems share a common optimal solution. Given the variables $y^{A,l}$ in P7, the variables $y_i^{B,l}$ in P1 can be constructed by:

$$y_i^{B,l} = \sum_{A \subset N: A \cap N_i = B} y^{A,l}, \quad \forall i \in N, B \subset N_i, l \in L. \quad (47)$$

Hence (P1c) becomes (P7c). Suppose all constraints in P7 hold. Then (P1f) is given by (47) and (P7e). For any nonempty

⁹In P7, the constraint (P7f) can be derived from (P6d) and (P6h).

set C such that $C \subset N_i \cap N_m$, we also have:

$$\sum_{B \subset N_i: B \cap N_m = C} y_i^{B,l} = \sum_{B \subset N_i: B \cap N_m = C} \sum_{A \subset N: A \cap N_i = B} y^{A,l} \quad (48)$$

$$= \sum_{A \subset N: A \cap N_i \cap N_m = C} y^{A,l} \quad (49)$$

$$= \sum_{B \subset N_m: B \cap N_i = C} \sum_{A \subset N: A \cap N_m = B} y^{A,l} \quad (50)$$

$$= \sum_{B \subset N_m: B \cap N_i = C} y_m^{B,l} \quad (51)$$

which implies (P1d). Moreover, (47) also suggests:

$$\sum_{B \subset N_i} y_i^{B,l} = \sum_{B \subset N_i} \sum_{A \subset N: A \cap N_i = B} y^{A,l} \quad (52)$$

$$= \sum_{A \subset N} y^{A,l} \quad (53)$$

$$= h^l. \quad (54)$$

Hence (P1e) is satisfied. Similarly, (P1f) is established as:

$$\sum_{B \subset N_i} |y_i^{B,l}|_0 = \sum_{B \subset N_i} \left| \sum_{A \subset N: A \cap N_i = B} y^{A,l} \right|_0 \quad (55)$$

$$\leq \sum_{B \subset N_i} \sum_{A \subset N: A \cap N_i = B} |y^{A,l}|_0 \quad (56)$$

$$\leq \sum_{A \subset N} |y^{A,l}|_0 \quad (57)$$

$$\leq 1. \quad (58)$$

Therefore, any solution in the feasible set of P7 will be a feasible solution to P1, i.e., the feasible set of P1 includes that of P7.

It remains to show the optimal solution to P1 belongs to the feasible set of P7. The key is to reconstruct global variables $y^{A,l}$ from the local variables $y_i^{B,l}$. Let us focus on a specific segment $l \in L$. Constraint (P1f) dictates that there is at most one active local pattern in each local cluster N_i . That is to say we can identify one active pattern $B_i^l \subset N_i$ for every AP $i \in N$, such that $y_i^{B,l} = 0, \forall B \neq B_i^l$. In fact all these active patterns from each AP's local cluster will be assigned the same bandwidth on the same segment l , i.e., $y_i^{B_i^l,l} = y_m^{B_m^l,l}, \forall i, m \in N, \forall l \in L$. If the two local patterns satisfy $B_i^l \cap N_m = B_m^l \cap N_i \neq \emptyset$, we must have $y_i^{B_i^l,l} = y_m^{B_m^l,l}$ according to (P1d). Therefore, the APs on a segment l are divided into groups of interfering APs. In each group, all the APs will assign the same bandwidth to its local active pattern. We can also see the bandwidths assigned to different groups are all equal to h^l in an optimal solution. This is because, if one group assign less than h^l bandwidth, we can proportionally scale up the nonzero y and z variables in this group until the y variables reach h^l . After such update, the solution is still feasible and the utility is improved. Hence all local active patterns on each segment l corresponds to a common global pattern:

$$A_l = \cup_{i \in N} B_i^l \quad \forall l \in L. \quad (59)$$

The bandwidth assigned to this active global pattern is h^l , which suggests the global variables are given by:

$$y^{A,l} = \begin{cases} h^l & \text{if } A = A_l \\ 0 & \text{otherwise} \end{cases} \quad (60)$$

It is easy to verify $(y^{A,l})_{A \subset N, l \in L}$ satisfies (P7c)-(P7f). Hence, the optimal solution to P1 is in the feasible set of P7. The equivalence is therefore established. ■

Propositions 2–5 imply that P0, P5, P6, P7, and P1 are all equivalent. Hence the proof of Theorem 1.

ACKNOWLEDGMENT

The authors thank Dr. Weimin Xiao and Dr. Jialing Liu for stimulating discussions.

REFERENCES

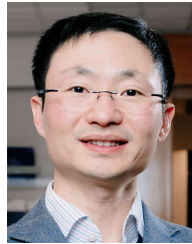
- [1] 3GPP TR 36.814, "Further advancements for E-UTRA physical layer aspects," v0.2.0, Nov. 2012.
- [2] I. Hwang, B. Song, and S. S. Soliman, "A holistic view on hyperdense heterogeneous and small cell networks," *IEEE Communications Magazine*, vol. 51, no. 6, pp. 20–27, 2013.
- [3] T. Nakamura, S. Nagata, A. Benjebbour, Y. Kishiyama, T. Hai, S. Xiaodong, Y. Ning, and L. Nan, "Trends in small cell enhancements in LTE advanced," *IEEE Communications Magazine*, vol. 51, no. 2, pp. 98–105, 2013.
- [4] W. Yu, T. Kwon, and C. Shin, "Multicell coordination via joint scheduling, beamforming, and power spectrum adaptation," *IEEE Trans. Wireless Commun.*, vol. 12, no. 7, pp. 1–14, 2013.
- [5] P. Frank, A. Müller, H. Droste, and J. Speidel, "Cooperative interference-aware joint scheduling for the 3GPP LTE uplink," in *21st Annual IEEE International Symposium on Personal, Indoor and Mobile Radio Communications*, pp. 2216–2221, IEEE, 2010.
- [6] F. Wang, L. Song, Z. Han, Q. Zhao, and X. Wang, "Joint scheduling and resource allocation for device-to-device underlay communication," in *Proc. Conf. Wireless Comm. and Networking*, pp. 134–139, IEEE, 2013.
- [7] A. Stolyar and H. Viswanathan, "Self-organizing dynamic fractional frequency reuse in OFDMA systems," in *Proc. IEEE INFOCOM*, pp. 691–699, Apr. 2008.
- [8] R. Chang, Z. Tao, J. Zhang, and C.-C. Kuo, "Multicell OFDMA downlink resource allocation using a graphic framework," *IEEE Trans. Veh. Technol.*, vol. 58, pp. 3494–3507, Sept 2009.
- [9] S. Ali and V. C. M. Leung, "Dynamic frequency allocation in fractional frequency reused OFDMA networks," *IEEE Trans. Wireless Commun.*, vol. 8, pp. 4286–4295, Aug. 2009.
- [10] R. Madan, J. Borran, A. Sampath, N. Bhushan, A. Khandekar, and T. Ji, "Cell association and interference coordination in heterogeneous LTE-A cellular networks," *IEEE J. Sel. Areas Commun.*, vol. 28, pp. 1479–1489, Dec. 2010.
- [11] W.-C. Liao, M. Hong, Y.-F. Liu, and Z.-Q. Luo, "Base station activation and linear transceiver design for optimal resource management in heterogeneous networks," *IEEE Trans. Signal Process.*, vol. 62, no. 15, pp. 3939–3952, 2014.
- [12] Z. Fang, X. Wang, and X. Yuan, "Joint base station activation and downlink beamforming design for heterogeneous networks," in *Global Communications Conference (GLOBECOM), 2015 IEEE*, pp. 1–6, IEEE, 2015.
- [13] A. Khandekar, N. Bhushan, J. Tingfang, and V. Vanghi, "LTE-advanced: Heterogeneous networks," in *2010 European Wireless Conference*, pp. 978–982, April 2010.
- [14] A. Damnjanovic, J. Montojo, Y. Wei, T. Ji, T. Luo, M. Vajapeyam, T. Yoo, O. Song, and D. Malladi, "A survey on 3GPP heterogeneous networks," *IEEE Trans. Wireless Commun.*, vol. 18, pp. 10–21, June 2011.
- [15] K. Shen and W. Yu, "Distributed pricing-based user association for downlink heterogeneous cellular networks," *IEEE J. Sel. Areas Commun.*, vol. 32, pp. 1100–1113, June 2014.
- [16] D. Fooladivanda and C. Rosenberg, "Joint resource allocation and user association for heterogeneous wireless cellular networks," *IEEE Trans. Wireless Commun.*, vol. 12, pp. 248–257, January 2013.

- [17] M. Hong and Z.-Q. Luo, "Distributed linear precoder optimization and base station selection for an uplink heterogeneous network," *IEEE Trans. Signal Process.*, vol. 61, pp. 3214–3228, June 2013.
- [18] Q. Kuang, J. Speidel, and H. Droste, "Joint base-station association, channel assignment, beamforming and power control in heterogeneous networks," in *Proc. IEEE 75th Vehicular Technology Conf. (VTC Spring)*, pp. 1–5, May 2012.
- [19] Y. Lin and W. Yu, "Optimizing user association and frequency reuse for heterogeneous network under stochastic model," in *Proc. IEEE GLOBECOM*, pp. 2045–2050, Dec 2013.
- [20] Q. Ye, B. Rong, Y. Chen, M. Al-Shalash, C. Caramanis, and J. Andrews, "User association for load balancing in heterogeneous cellular networks," *IEEE Trans. Wireless Commun.*, vol. 12, pp. 2706–2716, Jun. 2013.
- [21] B. Zhuang, D. Guo, and M. L. Honig, "Traffic-driven spectrum allocation in heterogeneous networks," *IEEE J. Sel. Areas Commun. Special Issue on Recent Advances in Heterogeneous Cellular Networks*, vol. 33, no. 10, pp. 2027–2038, 2015.
- [22] B. Zhuang, D. Guo, and M. L. Honig, "Energy-efficient cell activation, user association, and spectrum allocation in heterogeneous networks," *IEEE J. Sel. Areas Commun. Special Issue on Energy-Efficient Techniques for 5G Wireless Communication Systems*, vol. 34, no. 4, pp. 823–831, 2016.
- [23] B. Zhuang, D. Guo, E. Wei, and M. L. Honig, "Scalable spectrum allocation and user association in networks with many small cells," *IEEE Trans. Commun.*, vol. 65, no. 7, pp. 2931–2942, 2017.
- [24] Q. Kuang, W. Utschick, and A. Dotzler, "Optimal joint user association and multi-pattern resource allocation in heterogeneous networks," *IEEE Trans. Signal Process.*, vol. 64, pp. 3388–3401, July 2016.
- [25] Q. Kuang and W. Utschick, "Energy management in heterogeneous networks with cell activation, user association, and interference coordination," *IEEE Transactions on Wireless Communications*, vol. 15, pp. 3868–3879, June 2016.
- [26] Z. Zhou, D. Guo, and M. L. Honig, "Licensed and unlicensed spectrum allocation in heterogeneous networks," *IEEE Trans. Commun.*, vol. 65, pp. 1815–1827, 2017.
- [27] F. Teng and D. Guo, "Resource management in 5G: a tale of two timescales," in *Proc. Asilomar Conf. Signals, Systems, & Computers*, Pacific Grove, CA, USA, 2015.
- [28] E. J. Candés, M. B. Wakin, and S. P. Boyd, "Enhancing sparsity by reweighted l_1 minimization," *Journal of Fourier analysis and applications*, vol. 14, no. 5-6, pp. 877–905, 2008.
- [29] S. Boyd, N. Parikh, E. Chu, B. Peleato, and J. Eckstein, "Distributed optimization and statistical learning via the alternating direction method of multipliers," *Foundations and Trends® in Machine Learning*, vol. 3, no. 1, pp. 1–122, 2011.
- [30] K. Shen and W. Yu, "FPLinQ: A cooperative spectrum sharing strategy for device-to-device communications," in *Proc. of IEEE International Symposium on Information Theory*, pp. 2323–2327, 2017.
- [31] J. Li and D. Guo, "Cloud-based resource allocation and cooperative transmission in large cellular networks," in *Proc. Allerton Conf. Commun., Control, & Computing*, 2017.
- [32] M. Fortin and R. Glowinski, "Chapter III on decomposition-coordination methods using an augmented lagrangian," *Studies in Mathematics and Its Applications*, vol. 15, pp. 97–146, 1983.
- [33] D. Gabay, "Chapter IX applications of the method of multipliers to variational inequalities," *Studies in mathematics and its applications*, vol. 15, pp. 299–331, 1983.

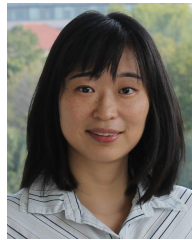


Binnan Zhuang received his B.S. degree from Electronic Engineering Department of Tsinghua University, Beijing, China, in 2009, the M.S. and Ph.D. degrees in electrical engineering from Northwestern University, Evanston, IL, USA, in 2010 and 2015, respectively. He is currently working as a staff engineer in the System on Chip (SoC) Lab of Samsung Semiconductor Inc. in San Diego, CA, USA. His research interests include wireless communications, communication network and network optimization. His current research at Samsung focus on computer

vision and communication.



Dongning Guo (S'97-M'05-SM'11) received the Ph.D. degree from Princeton University, Princeton, NJ. In 2004, he joined the faculty of Northwestern University, Evanston, IL, where he is currently a Professor in the Department of Electrical Engineering and Computer Science. He has been an Associate Editor of IEEE Transactions on Information Theory and a Guest Editor of a Special Issue of IEEE Journal on Selected Areas in Communications. He is an Editor of Foundations and Trends in Communications and Information Theory. Dr. Guo received the IEEE Marconi Prize Paper Award in Wireless Communications in 2010 and a Best Paper Award at the 2017 IEEE Wireless Communications and Networking Conference. He is also the recipient of the National Science Foundation Faculty Early Career Development (CAREER) Award in 2007.



Ermin Wei is currently an Assistant Professor at the EECS Dept of Northwestern University. She completed her PhD studies in Electrical Engineering and Computer Science at MIT in 2014, advised by Professor Asu Ozdaglar, where she also obtained her M.S.. She received her undergraduate triple degree in Computer Engineering, Finance and Mathematics with a minor in German, from University of Maryland, College Park. Wei has received many awards, including the Graduate Women of Excellence Award, second place prize in Ernst A. Guillemin Thesis Award and Alpha Lambda Delta National Academic Honor Society Betty Jo Budson Fellowship. Wei's research interests include distributed optimization methods, convex optimization and analysis, smart grid, communication systems and energy networks and market economic analysis.



Michael L. Honig (S'80-M'81-SM'92-F'97) received the B.S. degree in electrical engineering from Stanford University in 1977, and the M.S. and Ph.D. degrees in electrical engineering from the University of California, Berkeley, in 1978 and 1981, respectively. He subsequently joined Bell Laboratories in Holmdel, NJ, where he worked on local area networks and voiceband data transmission. In 1983 he joined the Systems Principles Research Division at Bellcore, where he worked on Digital Subscriber Lines and wireless communications. Since the Fall of 1994, he has been with Northwestern University where he is a Professor in the Department of Electrical and Computer Engineering. He has held several visiting scholar positions and has also worked as a freelance trombonist.

Dr. Honig has served as an Editor for the IEEE Transactions on Information Theory and the IEEE Transactions on Communications, and as Guest Editor for several journals. He has also served as a member of the Board of Governors for the Information Theory Society. He is the recipient of a Humboldt Research Award for Senior U.S. Scientists, and the co-recipient of the 2002 IEEE Communications Society and Information Theory Society Joint Paper Award and the 2010 IEEE Marconi Prize Paper Award.